Cell

EXTENDED EXPERIMENTAL PROCEDURES

Generation of Crfr2α-eGFPCre BAC Transgenic Mice

A mouse bacterial artificial chromosome (BAC clone RP23-78P13) containing the entire *Crfr2* gene was treated as follows to prepare it for the generation of transgenic mice. First, RecA-mediated homologous recombination (Yang et al., 1997) was used to disrupt expression of *Inmt*, a gene present on the BAC and known to be expressed in the brain; this step was taken to prevent a gain-of-function phenotype that could arise when a gene is overexpressed by a multicopy transgene. Disruption of *Inmt* was accomplished by inserting a bovine growth hormone polyadenylation sequence (BGHpA) cassette into the 5′ end of the *Inmt* gene that removed the start codon; 5′ and 3′ homologous sequences (referred to as Box A and Box B, respectively) were amplified by PCR (Phusion DNA polymerase, New England Biolabs) and cloned into pBluescript (Stratagene) flanking the BGHpA cassette. Sequences used were as follows: Box A (nucleotides −698 to +9, relative to 5′ end of *Inmt* exon I: forward primer, 5′-GATCTCTGGTCCTCCTACTTCC-3′; reverse primer, 5′-AATTCTAGCCAGCCCACACAGCT-3′; Box B (nucleotides +10 to +790): forward primer, 5′-AGGGCAAGGTATA CATAGGAG-3′; reverse primer, 5′-AGTTCCTTGGCACCGAATGTCTGG-3′. The *Inmt* mutant version of the BAC was then subjected to a second round of recombineering to target the *Crfr2* gene, for which two splice variants have been described in rodents: 1) a broadly expressed variant that is not highly expressed in brain (*Crfr2*β, ATG in exon I), and 2) a neuronally expressed form that is enriched in the brain and present at high levels in LS (*Crfr2*α, ATG in exon III) (Lovenberg et al., 1995; Chen et al., 2005). To simultaneously target *Crfr2*α and suppress expression *Crfr2*β from the BAC, two features were incorporated into the targeting vector: 1) a cassette containing an eGFPCre fusion gene followed by an SV40pA was inserted into the 5′UTR of the third exon of the *Crfr2* gene; 2) a STOP codon was introduced into exon IV (shared by both α and β splice forms) to terminate translation of any *Crfr2*β mRNA transcribed from the BAC. Sequences used were as follows: Box A (nucleotides −532 to +132, relative to 5′ end of *Crfr2* exon III: forward primer, 5′-TTCCTAGATGTCCTCCTCTCACC-3′; reverse primer, 5′-CCCCGGAGCCGCGCG; Box B (nucleotides +149 to +790): forward primer, 5′-CGGCGCTGCTCCTCAGCCTGC-3′; reverse primer, 5′-ACTTCAACAAACAGCGTAGAGGAAGG-3′. The final recombineered BAC containing the desired modifications was linearized with NotI, purified away from smaller fragments released by digestion (vector backbone plus genomic sequences located more than 85 kb upstream of the *Crfr2*α ATG) using a Sepharose CL4b column, integrity confirmed by pulsed field gel electrophoresis, and then microinjected into the pronuclei of FVB/N embryos to generate transgenic mice.

Animal Maintenance

The *Crfr2*α-eGFPCre BAC transgene was maintained on an FVB/N (Taconic) background. For all behavior experiments, hemizygous transgenic FVB/N males were bred to C57BL/6N (Harlan Sprague Dawley) females, and FVBB6F1 male mice were used for testing. All animals were housed at 23°C with *ad libitum* access to food and water in a 13-h day/11-h night cycle, with the day starting at 21:00. All behavioral testing was done during the dark cycle, starting no earlier than 11:00 and no later than 20:00. Following surgery, mice were singly housed prior to behavioral testing. We note that quantitative differences in behavioral results might be obtained on an inbred C57BL/6 congenic background. All experiments were conducted in accordance with NIH guidelines and approved by the Caltech Institutional Animal Care and Use Committee.

In Situ Hybridization

Single color ISH for *Crfr2* was performed on 120 μm thick free floating sections as described previously (Mongeau et al., 2003). In brief, brains were collected, cut in 3–4 mm coronal slabs using a block, and fixed overnight in 4% paraformaldehyde. Next, 120 μm-thick coronal sections were made from the tissue slabs using a vibratome, followed by gentle digestion for 30 min using proteinase K, fixation with 4% paraformaldehyde, and hybridization at 60°C overnight with a cRNA digoxigenin-labeled probe against *Crfr2* mRNA. Nonhybridized probe was washed off at 60°C and digested with RNase A at 37°C for 30 min. Immunohistochemistry was performed using antidigoxigenin conjugated with alkaline phosphatase (Roche), and development performed with the alkaline phosphatase substrate NBT/BCIP. Double-label fluorescent ISH (dFISH) protocols have been previously described in detail (Thompson et al., 2008). In brief, dFISH was performed using a variation of the colorimetric protocol. Briefly, riboprobes were labeled with either digoxigenin-UTP or dinitrophenyl-11-UTP (DNP; Perkin Elmer). A DNP-labeled probe and a DIG-labeled probe were hybridized simultaneously to 25 μm thick sections. Tyramide signal amplification was performed for each probe individually, using either anti-DIG-HRP with tyramide-biotin, or anti-DNP-HRP with tyramide-DNP for amplification. Visualization of signal was achieved using either streptavidin-Alexa Fluor 488 (Invitrogen/Molecular Probes) or anti-DNP-Alexa Fluor 555 (Invitrogen/Molecular Probes), and imaging performed on an Olympus FluoView-1000 confocal microscope. Regions used for probes are as follows: Cre recombinase, nucleotides 489-1441 (GenBank: X03453.1); *Crfr2*, nucleotides 459-1270 (NCBI Reference Sequence: NM_009953.3); *Esr1*, nucleotides 1123-2102 (GenBank: AB560752.1); *Gad2*, nucleotides 1069-2094 (NCBI Reference Sequence: NM_008078.2); *Penk*, nucleotides 312-1127 (NCBI Reference Sequence: NM_001002927.2); tdTomato, nucleotides 25-639 and 751-1365 (GenBank: AY678269.1); due to high homology, Cherry ISH was performed using the tdTomato probe.

Immunofluorescent Labeling

For immunostaining of free floating sections, mice were perfused transcardially with 0.9% saline followed by 4% paraformaldehyde (PFA) in 1× PBS. Brains were then removed and postfixed 16 hr at 4°C, washed in 1× PBS, and embedded in 3% low melting agarose

for vibratome sectioning at 75–100 μm. For immunostaining, sections were blocked in "NDS block" (5% normal donkey serum, 0.1% Triton X-100 in 1× PBS) for a minimum of 30' at room temperature, and primary antibodies diluted in NDS block and incubated 16 hr at 4°C. Following this, sections were washed 3× in PBS-T (0.1% Triton X-100 in 1× PBS), and incubated for 1–2 hr at room temperature in fluorescent secondary antibodies (Jackson Immunoresearch) diluted 1:1,000 in PBS-T. After this incubation, sections were washed, counterstained with 4',6-diamidino-2-phenylindole (DAPI), mounted, and coverslipped using either ProLong Gold Antifade Reagent (Invitrogen) or Fluoro Gel (Electron Microscopy Sciences). Cryosection immunostaining was performed similarly, with the following differences. After perfusion, brains were postfixed in 4% PFA for 1–2 hr on ice, followed by cryoprotection overnight at 4°C in 15% sucrose in 1× PBS, embedding in OCT, cryosectioning at 20 μm and collection onto Superfrost Plus slides (Ted Pella). Prior to immunostaining, sections were washed once in 1× PBS, and then postfixed for 5 min in cold methanol. Immunostaining then proceeding as detailed above for floating sections. Antibodies used were as follows: rabbit anti-Cre (Covance #PRB-106C **note*: the lot used in this study is no longer available and newer lots have not worked for IHC), goat anti-CTB (List #703), chicken anti-eGFP (Abcam #ab13970), rabbit anti-ESR1 (Santa Cruz #sc-542), and rabbit anti-UCN3 (Cosmo Bio Co #YII-Y364-EX). Secondary immunoreagents were obtained from Jackson Immunoresearch and Invitrogen. Fluorescent nuclear counterstaining was performed using 4',6-diamidino-2-phenylindole (DAPI).

Cell Counting

DAPI-counterstained sections were imaged on an Olympus FluoView-1000 confocal microscope, and cell counts performed using MetaMorph (Molecular Devices) in combination with manual scoring to ensure accuracy. Details on the specific regions quantitated are given in the relevant figure legends.

Cre-Dependent Viral Vectors

Viral plasmids encoding Cre-dependent opsins were provided by the Deisseroth (AAV-EF1a-DIO-hChR2(H134R)-EYFP, AAV-EF1a-DIO-eNpHR2.0-EYFP) and Boyden (AAV-CAGΔ-ArchT-GFP-FLEx) laboratories and packaged in serotype AAV5 at the University of Pennsylvania (U Penn) Gene Therapy Vector Core (ChR2-YFP and ArchT-GFP) or Harvard Gene Therapy Initiative (HGTI, eNpHR2.0-YFP). AAV5 encoding Cre-dependent ChR2-tdTomato was purchased from U Penn Vector Core inventory (lot #V1345). Cre-dependent AAV plasmid expressing humanized renilla GFP (hrGFP) was a gift from Clif Saper and was packaged in AAV5 at HGTI. Cre-dependent AAV5 expressing eYFP was purchased from the University of North Carolina (UNC) Gene Therapy Department stock inventory (AAV-EF1a-DIO-EYFP). AAV5 containing a CMV-Cre cassette was purchased from Vector Biolabs. A Cre-dependent nuclear-localized mCherry construct was generated by fusing a 3x nuclear localization sequence to mCherry and cloning this in place of ChR2-YFP in the vector EF1a-DIO-hChR2(H134R)-EYFP; packaging of this construct in AAV5 was done at U Penn. Construction, packaging, and validation of the Cre-dependent HSV129 variant HSV129ΔTK-TT has been previously described (Lo and Anderson, 2011). HSV129ΔTK-TT anterograde spread and labeling (tdT) are initiated only in Cre^+ "starter" cells; once rendered replication-competent in starter cells, the virus is able to propagate in the anterograde direction through downstream nodes of a given circuit.

Electrophysiological Slice Recordings

Standard mouse brain slice preparation and whole-cell recording were performed as follows: 3-5 month old mice were euthanized and coronal brain sections 250 μm thick were cut on a Vibratome (VT1000S; Leica) in ice-cold glycerol-based artificial cerebrospinal fluid (composition in mM: 252 glycerol, 1.6 KCl, 1.2 NaH_2PO_4, 1.2 $MgCl_2$, 2.4 $CaCl_2$, 18 $NaHCO_3$, 11 glucose, oxygenated with 95% O_2/5% CO_2). Slices were allowed to recover for 90 min at 32°C in standard artificial cerebrospinal fluid (ACSF; composition in mM: 126 NaCl, 1.6 KCl, 1.2 NaH_2PO_4, 1.2 $MgCl_2$, 2.4 $CaCl_2$, 18 $NaHCO_3$, 11 glucose, oxygenated with 95% O_2/5% CO_2). After this recovery period, slices were then transferred to room temperature oxygenated ACSF where they remained until recording. Cells expressing GFP or YFP were detected by infrared differential interference contrast (IR-DIC) and fluorescence video microscopy (Olympus BX51). Whole-cell voltage and current clamp recordings were performed at 30°C with a MultiClamp 700B amplifier and Digidata 1440A (Molecular Devices). The patch pipette, with a resistance of 7–9 MΩ,was filled with an intracellular solution containing (in mM) 135 potassium gluconate, 5 EGTA, 0.5 $CaCl_2$,2$MgCl_2$, 10 HEPES, 2 MgATP and 0.1GTP, pH7.2, 280–300 mosM. Series resistance was typically 20–30 MΩ. Cell attached recordings were performed in voltage clamp with holding current maintained at zero, and using pipettes filled with ACSF. Appropriate bridge balance was applied to all current clamp recordings. Data were sampled at 10 kHz, filtered at 3 kHz and analyzed with pCLAMP10 or Igor Pro (Wavemetrics) using the Neuromatic analysis software package written by Jason Rothman (http://neuromatic.thinkrandom.com/).

Stereotaxic Surgery

Mice 2–5 months old were anaesthetized 2.5% isoflurane, placed into a stereotaxic frame (Kopf Model 940), and anesthesia maintained using 1%–1.5% isoflurane. To enhance uptake of pressure injected solutions, animals were injected with 0.4 ml of 20% mannitol (Phoenix Pharmaceuticals). The skull was exposed and holes produced using with a hand-held drill (Roboz) with 0.7mm bits (Fine Science Tools). Injections were targeted using coordinates based on the Paxinos and Franklin mouse brain atlas (Paxinos and Franklin, 2001), relative to bregma (LS, AP+0.5, ML ± 0.59,DV-2.8; AHA, AP-0.8, ML ± 0.3, DV-4.9; LH, AP-1.6, ML ± 0.9, DV-5.25). Virus was backfilled into glass capillaries (tip diameter ~50 μm) and delivered at a rate of 30 nl per minute using a nanoliter injector (Nanoliter 2000, World Precision Instruments) controlled by an ultra microsyringe pump (Micro4, World Precision

Instruments). Volumes delivered were between 50–100 nl, amounts determined empirically to be the largest that would label cells in LS without spread to and recombination in adjacent brain regions. AAV molecular titers were on the order of ~3E+12, resulting in a total ~3E+8 total viral particles delivered per injection site. If needed, bilateral stainless steel guide cannulas (Plastics1) were implanted above the injection sites; lengths of tubing below pedestal were: LS, 2.6 mm; AHA, 4.2 mm. After implantation, bilateral stylets were inserted into the guides to prevent clogging. For optogenetic manipulations of LS *Crfr2α*$^+$ axons in the hypothalamus, bilateral stainless steel guide cannulas were implanted with tips located 1.5 mm posterior and 1.5 mm ventral to the virus injection sites in LS and which extended down to approximately 500 μm above the medial hypothalamus at the level of the AHA. For postoperative care, mice were injected subcutaneously with ketoprofen (2 mg per kg body weight) and supplied for 7 days with drinking water containing 400 mg/l sulphamethoxazole and 200 mg/l ibuprofen. Mice were given four (eNpHR2.0 and ArchT) or six (ChR2) weeks after injection to allow for viral expression before being used for behavior experiments. All surgically manipulated animals underwent histological examination to ensure proper guide placement and/or that viral expression was restricted to the LS.

In Vivo Optogenetic Control of Neuronal Activity

To enable in vivo delivery of light, custom bilateral fiber assemblies were built by inserting two 200 μm optic fibers (0.37 NA multimode fiber, Thorlabs) through plastic bilateral guide pedestals (from which the steel tubing had been removed), gluing them in place, and then cutting the ends so that the tips of the fibers would be flush with the tips of implanted stainless steel guides in the brains of mice. On the day of testing, mice were anesthetized with isoflurane, stylets were removed and a bilateral fiber assembly was connected by inserting one end into the guide (held in place using dust caps (Plastics1)) and the other end connected via FC/PC to a 1 × 2 intensity division fiber optic rotary joint (Doric Lenses) that was suspended above the test arenas using a boom microphone stand (Proline). Two mice were tested at the same time by connecting two rotary joints to a beam splitter (1 × 2 intensity division minicube, Doric Lenses) that was in turn connected to lasers (473 nm, 532 nm, or 59 nm, Shanghai Laser & Optics Century) located outside the testing room and which were controlled by a pulse stimulator (A310 Accupulser Signal Generator, World Precision Instruments). Light power at the tips of the fibers were measured prior to insertion into mice using a power meter (Thorlabs).

Behavioral Testing

All behavioral testing was done using male *Crfr2α*-eGFPCre mice on an FVBB6F1 background. Animals were lightly anesthetized with 2% isoflurane prior to testing to allow insertion of fiber optic cables, which was done in the antechamber of the room where the animals were housed. To assay anxiety behavior, mice were tested sequentially in three standard assays, each lasting 10 min each: light-dark box (LDB), box dimensions 50 × 25 × 30 cm; light side 31 cm long, dark side 16 cm long; doorway between light and dark sides, 5.25 cm wide, 9 cm high), mice introduced into dark side at start of assay, parameters measured included number of entries into and time spent in light side; open field (OF), 50 × 50 × 30 boxes constructed from white 1/8" ABS white plastic, mice introduced into a corner at start of assay, parameters measured included number of entries into and time spent in a 17 × 17 cm square region in the "center" of the open field, total distance moved, and time spent immobile; novel object (NO), a stainless steel cup (base diameter 3.5 cm, lip diameter 5.75 cm, base to lip height = 4.5 cm) was placed in the center of the open field box, parameters measured included number of entries into and time spent exploring the object in a 17 × 17 cm square region in the "center" of the open field, total distance moved, and time spent immobile. Average velocity in the open field was calculated by dividing total distance moved by time spent mobile (Distance moved / Time in OF – time spent immobile). To avoid confounds from conditioning effects (i.e., conditioned fear instead of innate anxiety), separate groups of mice were injected and tested for each data set presented. The one exception to this is the data in Figure S2H (retesting ChR2-injected mice 7 days after stimulation); in that experiment, different novel objects were used in the second assay (6 × 6 × 1.25 cm plastic squares). For photoinhibition experiments involving stress, mice were subjected to 20 min of immobilization stress, an length of time determined empirically to be the minimum length necessary to elevate anxiety in FVBB6F1 mice (data not shown). Note that no differences were detected between groups in that experiment. All behavior experiments were captured in MPEG-2 (.m2v) format using Mediacruise (Canopus) and analyzed with Ethovision 3.1 (Noldus Information Technology). At the completion of behavioral testing, all mice were perfused and histologically analyzed to ensure viral expression was restricted to LS and guide cannulas were properly positioned. Procedures used for individual experiments were as follows:

Photostimulation of LS Crfr2α$^+$ Cells Using ChR2(H134R)-YFP during Testing in Naive Mice

Following insertion of optic fibers into guides, mice were placed in a new cage, transferred to the testing room and connected to a 1 × 2 rotary joint. After a 10 min period to recover from anesthesia, mice were run sequentially through the LDB, OF, and NO (10 min each assay) in the presence of 473 nm light (15 Hz, 20 ms pulse width, 5 s ON, 5 s off). For all ChR2 experiments, light power at the fiber tips was 380 mW/mm^2, which is sufficient to yield 1 mW/mm^2 (the minimum amount of light reported to be capable of efficient ChR2 activation; Aravanis et al., 2007) at 1.4 mm below the fiber tips and therefore should be capable of photostimulating the full dorsoventral span of LS *Crfr2α*$^+$ cell bodies.

Photostimulation of LS Crfr2α$^+$ Cells Using ChR2(H134R)-YFP prior to Testing in Naive Mice

Following insertion of optic fibers into guides, mice were transferred to a novel "stimulation" room and placed in a clean cage inside an open box that had been sprayed with a novel odor (Simple Green). After connection to a 1 × 2 rotary joint, mice received photostimulation with 473 nm light (15 Hz, 20 ms pulse width, 5 s ON, 5 s off) for 30 min. Following this, photostimulation was terminated,

optic fibers were removed, and stylets reinserted into the guides. All animals were then moved out of the stimulation room and into the testing room, and run through the anxiety test battery (LDB,OF,NO) as described above.

Photostimulation of LS Crfr2α+ Cells Using ChR2(H134R)-YFP during Stress prior to Testing

To minimize the potential confound of a ceiling effect (i.e., anxiety levels so high that no additional elevation is detectable in these assays), mice used for this experiment were habituated by handling 5 min per day for 3 days prior to testing in order to reduce sensitivity to stress. Following insertion of optic fibers into guides, mice were subjected to immobilization stress (IMS) by taping their limbs to a plastic tray using green lab tape (VWR); taping required ~30 s and was completed just as mice were awaking from isoflurane anesthesia. IMS was done in a biosafety cabinet for 30 min during which time mice received photostimulation with 473 nm light (15 Hz, 20 ms pulse width, 5 s ON, 5 s off). Following this 30 min period, optic fibers were removed, mice were released from IMS, and then transferred in a new cage to the testing room where they were then run through the anxiety test battery (LDB,OF,NO) as described above.

Photoinhibition of LS Crfr2α+ Cells Using eNpHR2.0-YFP during Stress prior to Testing

Following insertion of optic fibers into guides, mice were subjected to immobilization stress (IMS) in a biosafety cabinet for 20 min during which time they received illumination with 593 nm light (continuous light, 20 s ON, 10 s off). In all eNpHR2.0 experiments, light power at the fiber tips was 475 mW/mm^2. Following this 20 min period, optic fibers were removed, mice were released from IMS, and were then transferred in a new cage to the testing room where they were then run through the anxiety test battery (LDB,OF,NO) as described above.

Photoinhibition of LS Crfr2α+ Cells Using eNpHR2.0-YFP after Stress during Testing

Following insertion of optic fibers into guides, mice were subjected to immobilization stress (IMS) in a biosafety cabinet for 20 min. Following this 20 min period, mice were released from IMS and transferred in a new cage to the testing room. Fibers were connected to a 1 × 2 rotary joint, and mice were run through the anxiety test battery (LDB,OF,NO) as described above while receiving illumination with 593 nm light (continuous light, 20 s ON, 10 s off) throughout testing.

Photoinhibition of LS Crfr2α+ Cells Using eNpHR2.0-YFP during Testing in Naive Mice

Following insertion of optic fibers into guides, mice were transferred in a new cage to the testing room and connected to a 1 × 2 rotary joint. After a 10 min period to recover from anesthesia, mice were run sequentially through the LDB, OF, and NO, mice were run through the anxiety test battery (LDB,OF,NO) while receiving illumination with 593 nm light (continuous light, 20 s ON, 10 s off) throughout testing.

Photoinhibition of LS Crfr2α+ Projections to AHA Using ArchT-GFP after Stress during Testing

Following insertion of optic fibers into guides, mice were subjected to IMS in a biosafety cabinet for 20 min. Following this 20 min period, mice were released from IMS and transferred in a new cage to the testing room. Fibers were connected to a 1 × 2 rotary joint, and mice were run through the anxiety test battery (LDB,OF,NO) as described above while receiving illumination with 532 nm light (continuous light, 20 s ON, 10 s off) throughout testing. Light power at the fiber tips was 318 mW/mm^2.

Photostimulation of LS Crfr2α+ Terminals in AHA Using ChR2(H134R)-YFP during Testing in Naive Mice

Following insertion of optic fibers into guides, mice were placed in a new cage, transferred to the testing room, and connected to a 1 × 2 rotary joint. After a 10 min period to recover from anesthesia, mice were run sequentially through the LDB, OF, and NO (10 min each assay) in the presence of 473 nm light (15 Hz, 20 ms pulse width, 5 s ON, 5 s off).

Statistics

Responses to stress can vary widely, with some individuals showing robust and persistent elevations in anxiety behavior while others are relatively resilient and maintain normal functioning even following exposure to severe trauma (Russo et al., 2012). We observed large variations in susceptibility to immobilization stress among the mice tested, including the presence of resilient outliers that resulted in data sets that were nonnormally distributed (i.e., failed three different tests for normality: Kolmogorov-Smirnov, D'Agostino and Pearson omnibus normality test, and Shapiro-Wilk normality tests). For this reason, all data derived from stressed mice were plotted in box and whisker format (with whiskers representing minimum and maximum data points) and statistical significance assessed using nonparametric Mann-Whitney *U* tests. In contrast, data from unstressed mice generally passed at least one of the tests for normality and so were plotted as standard column bar graphs depicting mean ± SEM and analyzed for significance using unpaired t tests.

Channelrhodopsin-Assisted Circuit Mapping

Four to six weeks after injecting Cre-dependent ChR2(H134R)-YFP AAV5 into LS, brain slices were prepared for electrophysiological recordings as described above. Light from a 473 nm laser (Shanghai Dream Laser) was delivered via a 200 μm fiber optic cable positioned next to the region of interest using a micromanipulator. Light pulses (2 ms pulse width) were triggered using pClamp; synchronous with the triggering of the laser, a 200 μs depolarization of 1 mV was done to create an artifact that enabled determination of the precise time when the light pulse was initiated. Cells in whole-cell configuration were held in voltage clamp at −40 mV and identification of currents as being GABA-A-mediated was done using 100 μM picrotoxin. No postsynaptic excitatory currents were detected in response to stimulation of LS *Crfr2α*$^+$ neurons (0/66 cells). Onset of postsynaptic responses was determined using the Threshold method (Fedchyshyn and Wang, 2007), where IPSC onset was defined at the time point when the response reached 10% of its maximum. Latency to onset of a response was determined by subtracting the time point when the laser was triggered from the time point when onset of a PSC occurred.

Retrograde Tracing

For neuroanatomical studies using CTB, mice were prepared for stereotaxic surgery and CTB (0.5% in PBS, List) was iontophoretically delivered using alternating positive current (5 μA, 7 s ON, 7 s OFF) for 3 min using a Midgard Precision Current source (Stoelting). Following survival times of 5–7 days, mice were perfused and processed for immunostaining. For experiments involving CRACM combined with retrograde tracing, Cre-dependent ChR2-YFP AAV was injected into the LS of *Crfr2α*-eGFPCre mice. Following a 4 week viral incubation period, 20 nl of red retrobeads (diluted 1:4) were injected into the PVN (AP-0.4, ML+0.25, DV-4.5 to 4.4), and recordings performed 5 or 14 days later.

Corticosterone Measurements

Mice were injected and implanted as described above. To test effects of *Crfr2α*$^+$ neuronal stimulation in naive mice on circulating corticosterone levels, *Crfr2α*-eGFPCre male mice injected and implanted in LS with Cre-dependent ChR2-YFP AAV5 and guide cannulas respectively were anesthetized with 2% isoflurane and optic fibers inserted. Mice were transferred to a novel room and placed in a clean cage inside an open box. After connection to a 1 × 2 rotary joint, mice received photostimulation with 473 nm light (15 Hz, 20 ms pulse width, 5 s ON, 5 s off) for 30 min. Light power at the fiber tips was 380 mW/mm^2. Following this, photostimulation ceased and mice were immediately euthanized and decapitated (45–60 s following termination of photostimulation) for blood collection. To test the role of the LS *Crfr2α*$^+$ projection to the AHA in stress-induced elevation of corticosterone, *Crfr2α*-eGFPCre male mice injected in LS with Cre-dependent ArchT-GFP AAV5 and implanted with guide cannulas over the AHA were anesthetized with 2% isoflurane and optic fibers inserted. Mice were subjected to IMS in a biosafety cabinet for 20 min during which time they received illumination with 532 nm light (continuous light, 20 s ON, 10 s off). Light power at the fiber tips was 318 mW/mm^2. Following this, illumination ceased and mice were immediately euthanized and decapitated (45–60 s following termination of illumination) for blood collection. For both groups, blood was collected in 1.5 ml Eppendorf tubes and allowed to clot at room temperature for 10 min. Tubes were then spun at 2,000 *g* for 15 min to pellet cells, and supernatant containing clear serum removed and frozen on dry ice. Corticosterone concentrations were measured using an enzyme immunoassay kit (Cat#900-097, Enzo Life Sciences).

SUPPLEMENTAL REFERENCES

Aravanis, A.M., Wang, L.P., Zhang, F., Meltzer, L.A., Mogri, M.Z., Schneider, M.B., and Deisseroth, K. (2007). An optical neural interface: in vivo control of rodent motor cortex with integrated fiberoptic and optogenetic technology. J. Neural Eng. *4*, S143–S156.

Chen, A., Perrin, M., Brar, B., Li, C., Jamieson, P., Digruccio, M., Lewis, K., and Vale, W. (2005). Mouse corticotropin-releasing factor receptor type 2alpha gene: isolation, distribution, pharmacological characterization and regulation by stress and glucocorticoids. Mol. Endocrinol. *19*, 441–458.

Fedchyshyn, M.J., and Wang, L.Y. (2007). Activity-dependent changes in temporal components of neurotransmission at the juvenile mouse calyx of Held synapse. J. Physiol. *581*, 581–602.

Lo, L., and Anderson, D.J. (2011). A Cre-dependent, anterograde transsynaptic viral tracer for mapping output pathways of genetically marked neurons. Neuron *72*, 938–950.

Lovenberg, T.W., Chalmers, D.T., Liu, C., and De Souza, E.B. (1995). CRF2 alpha and CRF2 beta receptor mRNAs are differentially distributed between the rat central nervous system and peripheral tissues. Endocrinology *136*, 4139–4142.

Madisen, L., Zwingman, T.A., Sunkin, S.M., Oh, S.W., Zariwala, H.A., Gu, H., Ng, L.L., Palmiter, R.D., Hawrylycz, M.J., Jones, A.R., et al. (2010). A robust and high-throughput Cre reporting and characterization system for the whole mouse brain. Nat. Neurosci. *13*, 133–140.

Mongeau, R., Miller, G.A., Chiang, E., and Anderson, D.J. (2003). Neural correlates of competing fear behaviors evoked by an innately aversive stimulus. J. Neurosci. *23*, 3855–3868.

Paxinos, G., and Franklin, K.B.J. (2001). The Mouse Brain in Stereotaxic Coordinates (New York: Academic Press).

Russo, S.J., Murrough, J.W., Han, M.H., Charney, D.S., and Nestler, E.J. (2012). Neurobiology of resilience. Nat. Neurosci. *15*, 1475–1484.

Thompson, C.L., Pathak, S.D., Jeromin, A., Ng, L.L., MacPherson, C.R., Mortrud, M.T., Cusick, A., Riley, Z.L., Sunkin, S.M., Bernard, A., et al. (2008). Genomic anatomy of the hippocampus. Neuron *60*, 1010–1021.

Yang, X.W., Model, P., and Heintz, N. (1997). Homologous recombination based modification in Escherichia coli and germline transmission in transgenic mice of a bacterial artificial chromosome. Nat. Biotechnol. *15*, 859–865.

Yizhar, O., Fenno, L.E., Prigge, M., Schneider, F., Davidson, T.J., O'Shea, D.J., Sohal, V.S., Goshen, I., Finkelstein, J., Paz, J.T., et al. (2011). Neocortical excitation/inhibition balance in information processing and social dysfunction. Nature *477*, 171–178.

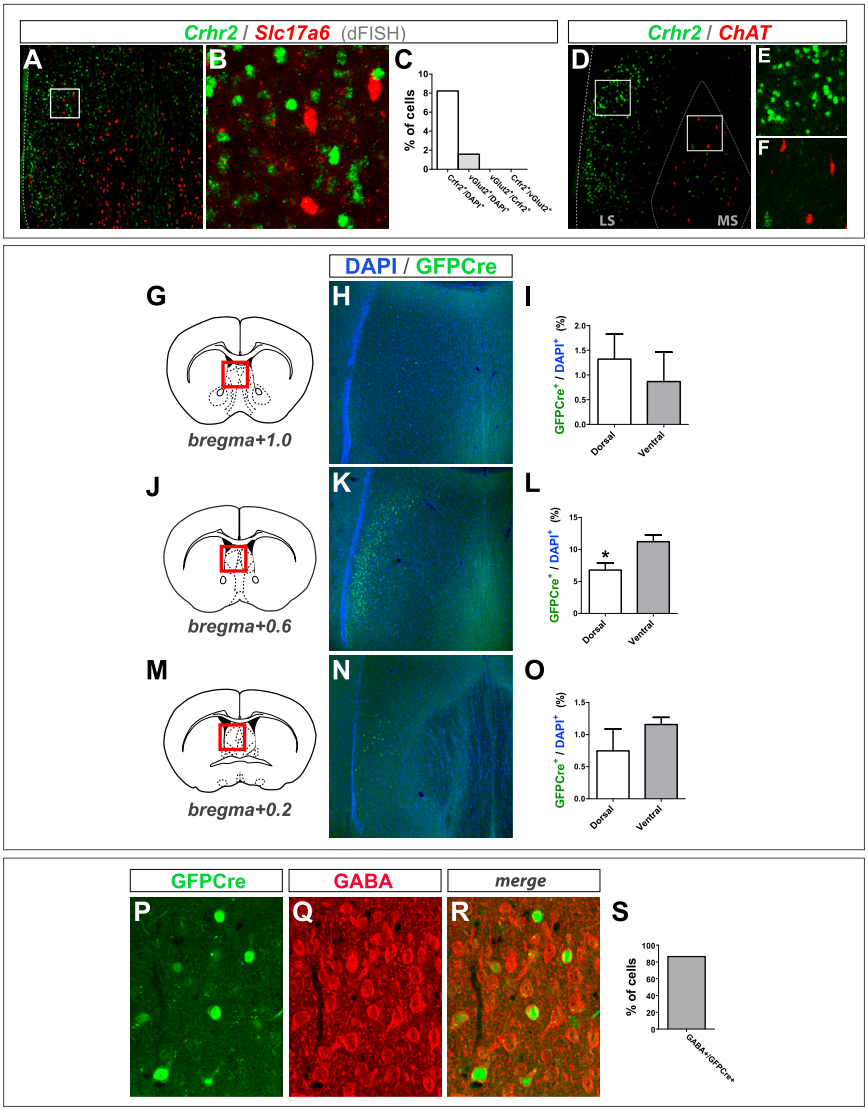

Figure S1. Additional Characterization of *Crfr2* mRNA and BAC Transgene Expression in LS, Related to Figure 2

(A and B) dFISH for *Crfr2* (green) versus the glutamatergic marker *Slc17a6* (a.k.a. *vGlut2*, red).

(C) No overlap is observed between *Crfr2* and *Slc17a6* in LS: *Crfr2*$^+$/DAPI$^+$ = 8.2%, *Slc17a6*$^+$/DAPI$^+$ = 1.6%, *Crfr2*$^+$/*Slc17a6*$^+$ = 0, *Slc17a6*$^+$/*Crfr2*$^+$ = 0; 8.2%x1.6%x11,221 DAPI$^+$ cells counted ~15 *Crfr2*$^+$*Slc17a6*$^+$ cells expected if expression were random; 0 *Crfr2*$^+$*Slc17a6*$^+$ cells were observed.

(D–F) dFISH for *Crfr2* (green) versus the cholinergic marker *ChAT* (red). We detected no *ChAT* expression in lateral septum, despite observing numerous *ChAT*$^+$ cells in other regions known to contain cholinergic neurons such as medial septum (MS in D,F), striatum, and basal forebrain (data not shown).

(G–O) Counts of eGFPCre$^+$ cells at three rostrocaudal levels of LS (G-I, bregma+1.0; J-L, bregma+0.6; M-O, bregma+0.2) revealed that, similar to endogenous *Crfr2* mRNA (main Figures 2A–2E), immunodetectable transgene expression is highest at middle LS levels (bregma+0.6), with fewer immunopositive neurons in more rostral and caudal regions. (I) Bregma+1.0, dorsal LS, eGFPCre$^+$/DAPI$^+$ = 1.3% ± 0.5%, n = 1,527 DAPI$^+$ cells; ventral LS, eGFPCre$^+$/DAPI$^+$ = 0.9% ± 0.6%, n = 1,828 DAPI$^+$ cells. (L) Bregma+0.6, dorsal LS, eGFPCre$^+$/DAPI$^+$ = 6.8% ± 2.0%, n = 1,932 DAPI$^+$ cells; ventral LS, eGFPCre$^+$/DAPI$^+$ = 11.2% ± 1.8%, n = 2,412 DAPI$^+$ cells. (O) Bregma+0.2, dorsal LS, eGFPCre$^+$/DAPI$^+$ = 0.8% ± 0.3%, n = 1,881 DAPI$^+$ cells; ventral LS, eGFPCre$^+$/DAPI$^+$ = 1.2% ± 0.1%, n = 2,525 DAPI$^+$ cells. Counts are mean ± SEM from 3 separate *Crfr2α*-eGFPCre transgenic mice.

(P–S) Immunostaining for BAC transgenic eGFPCre (green) and GABA (red), and quantitation; (S) 306/354 GFPCre$^+$ cells (86.4%) were GABA$^+$, which is similar the percentage of *Gad2*$^+$/*Crfr2*$^+$ cells detected using dFISH (main Figure 2F).

Finally, we note that in our Channelrhodopsin-assisted circuit mapping (CRACM) experiments in which ChR2 was expressed in LS *Crfr2α*$^+$ cells and recordings performed to identify *postsynaptic* targets, monosynaptic inhibitory postsynaptic currents (IPSCs) were detected in 44/66 cells (15/18 in LS, 29/48 in hypothalamus). However, excitatory postsynaptic currents were never detected (0/66 cells). Taken together, these data demonstrate that *Crfr2α*$^+$ neurons are a predominantly GABAergic, inhibitory population.

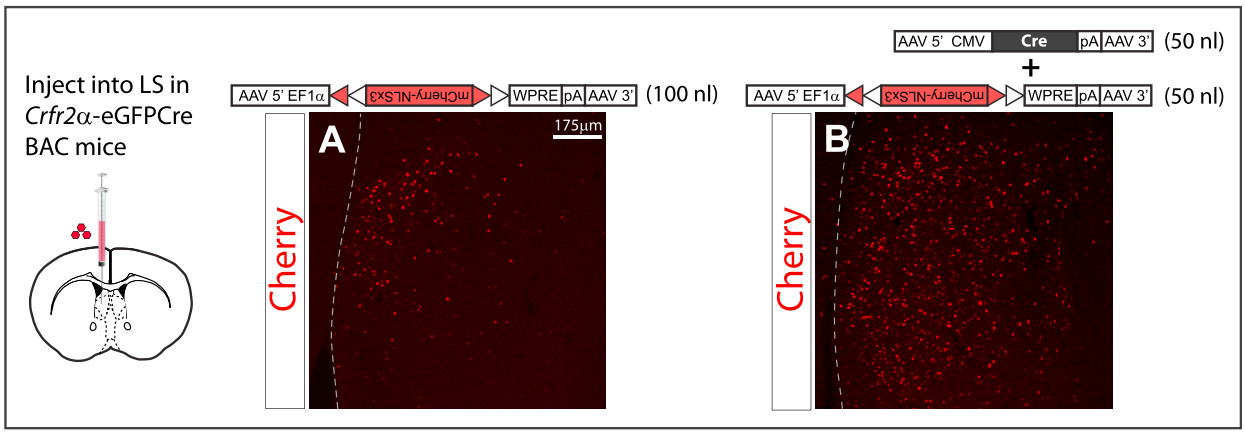

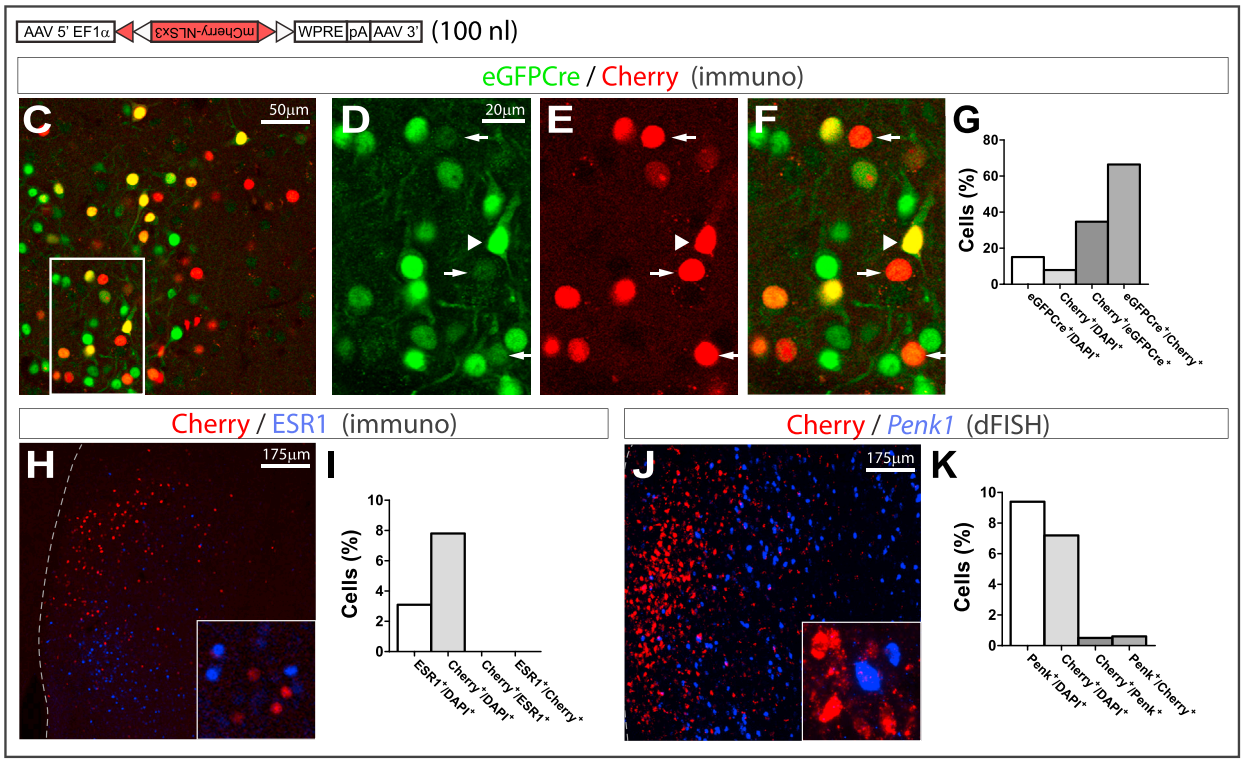

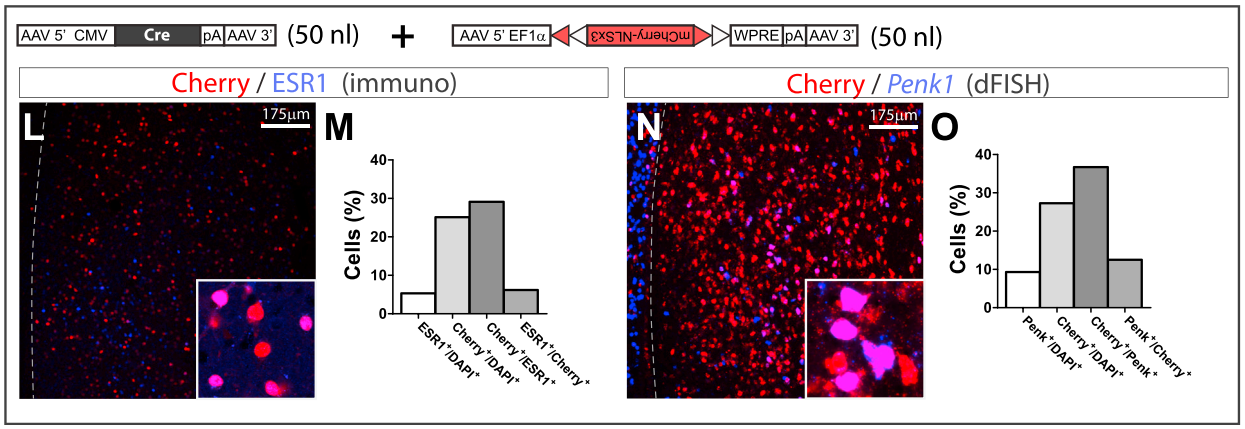

(legend on next page)

Figure S2. Injection of Cre-Dependent AAVs Employing the EF1α Promoter into *Crfr2α*-eGFPCre Mice Yields Specific Expression in *Crfr2α*$^+$ Neurons, Related to Figure 2

(A) Stereotaxic injection into the LS of *Crfr2α*-eGFPCre mice of a Cre-dependent AAV5 in which the EF1α promoter drives expression of a nuclear-targeted mCherry. Recombination is strongest in laterally situated neurons of LSi and LSv, with scattered Cherry$^+$ cells seen in medial LS. This pattern of recombination is similar to expression of endogenous *Crfr2* mRNA (Figure 1C in main text). Volume of AAV injected = 100 nl.

(B) Coinjection of the Cre-dependent Cherry construct together with a second AAV that constitutively expresses Cre recombinase was done to assess the labeling when recombination occurred in a large fraction of infected cells. In this case, no clear patterning is observed, with Cherry$^+$ cells detected throughout the LS. Moreover, the amount of Cre-dependent Cherry AAV in this experiment (50 nl) is half the volume injected in experiment shown in (A) and yet results in significantly more labeling. These data indicate that the pattern of recombination seen in (A) is a reflection of Cre activity and not due to an inability of AAV5 or the EF1α promoter to infect or express in LS neurons in general.

(C–G) Assessment of the sensitivity and specificity of Cre-dependent AAVs injected into LS of *Crfr2α*-eGFPCre mice. (C–F) Comparison of transgenically expressed eGFPCre (green) and virally expressed Cherry (red). Similar to what was observed with endogenous *Crhr2* mRNA (inset in Figure 1C of main text), the *Crfr2α*-eGFPCre transgene showed a broad dynamic range of expression, driving both low (arrows in C-F) and high (arrowhead in C-F) expression of eGFPCre, both of which were sufficient to catalyze recombination of the injected AAV. (G) Counts were performed in regions containing Cherry$^+$ cells: eGFPCre$^+$/DAPI$^+$ = 15.1%, Cherry$^+$/DAPI$^+$ = 7.9%, Cherry$^+$/eGFPCre$^+$ = 34.7%, eGFPCre$^+$/Cherry$^+$ = 66.4%; total n = 2,671 DAPI$^+$ cells

(H–K) Two factors complicate efforts to assess the specificity of recombination in transgenic or gene targeted mice that use cell type-specific promoters to express Cre. First, the ability of Cre to catalyze recombination even when present at very low levels can lead to labeling of cells in which the endogenous mRNA or protein under the regulation of the cell-specific promoter cannot be detected. This has been observed in gene targeted mouse lines (Madisen et al., 2010; Yizhar et al., 2011), suggesting it is a reflection of Cre sensitivity. Similarly and in the case of *Crfr2*, a second complicating factor is its broad dynamic range of expression and possibility of failure to detect message in low expressors when using dFISH (i.e., false negatives). We therefore used an indirect approach to further test specificity of recombination in *Crfr2α*-eGFPCre mice. We reasoned that if recombination were occurring randomly, it should be detected in LS populations that are known to be *Crfr2*-negative. We defined two such populations as those that express *Esr1* or *Penk* (Figures 2G–2J in main text), and so used immunostaining (H,I) or dFISH (J,K) to determine if any recombination had occurred in *Esr1*$^+$ (H,I) or *Penk*$^+$ (J,K) cells. This analysis revealed that significant recombination had not occurred in either of these two populations; counts were performed in regions containing Cherry$^+$ cells: Cherry versus ESR1: ESR1$^+$/DAPI$^+$ = 3.1%, Cherry$^+$/DAPI$^+$ = 7.8%, Cherry$^+$/ESR1$^+$ = 0, ESR1$^+$/Cherry$^+$ = 0; 3.1%x7.8%x1,645 cells counted = 4 Cherry$^+$ESR1$^+$ cells expected if recombination were random, 0 Cherry$^+$ESR1$^+$ cells were observed; Cherry versus *Penk*: *Penk*$^+$/DAPI$^+$ = 9.4%; Cherry$^+$/DAPI$^+$ = 7.2%, Cherry$^+$/*Penk*$^+$ = 0.5%, *Penk*$^+$/Cherry$^+$ = 0.6%; 9.4%x7.2%x7,187 cells counted = 49 Cherry$^+$/*Penk*$^+$ cells expected if expression were random; 3 Cherry$^+$*Penk*$^+$ cells were observed.

(L–O) Absence of significant recombination in ESR1$^+$ and *Penk*$^+$ cells is not due to the inability of AAV5 or the EF1α promoter to infect or express in these populations. Coinjection of the Cre-dependent Cherry AAV together with a CMV-Cre AAV resulted in Cherry expression in both ESR1$^+$ (L,M) and *Penk*$^+$ (N,O) cells near expected frequencies, counts were performed in regions containing Cherry$^+$ cells. (M) Cherry versus ESR1: ESR1$^+$/DAPI$^+$ = 5.3%, Cherry$^+$/DAPI$^+$ = 25.1%, Cherry$^+$/ESR1$^+$ = 29.1%, ESR1$^+$Cherry$^+$ = 6.2%; 5.3%x25.1%x2,780 cells counted = 37 Cherry$^+$ESR1$^+$ cells expected if recombination were random, 43 Cherry$^+$ESR1$^+$ cells were observed. (O) Cherry versus *Penk*: *Penk*$^+$/DAPI$^+$ = 9.3%, Cherry$^+$/DAPI$^+$ = 27.3%, Cherry$^+$/*Penk*$^+$ = 36.7%, *Penk*$^+$Cherry$^+$ = 12.5%; 9.3%x27.3%x5,061 cells counted = 128 Cherry$^+$/*Penk*$^+$ cells expected if expression were random; 172 Cherry$^+$*Penk*$^+$ cells were observed.

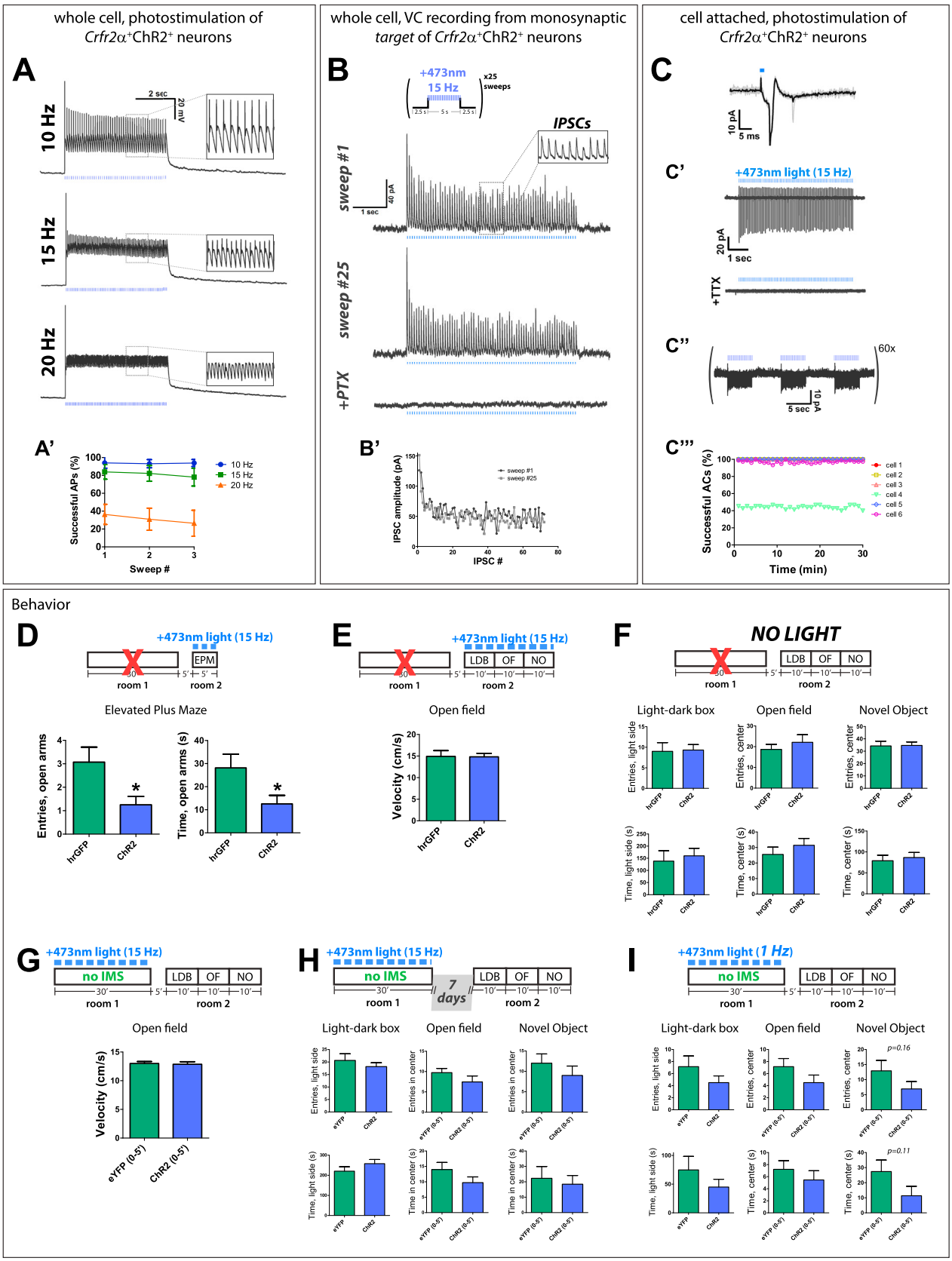

(legend on next page)

Figure S3. LS *Crfr2α*$^+$ Neuronal Responses to Optogenetic Stimulation and ChR2 Behavior Controls, Related to Figure 3

(A and B) To determine the maximal rates at which LS *Crfr2α*$^+$ neurons are capable of efficient firing in response to photostimulation, whole-cell recordings were performed on *Crfr2α*$^+$ChR2$^+$ cells in acute slices from *Crfr2α*-eGFPCre mice injected 4 weeks earlier with Cre-dependent ChR2 AAV. (A) Cells (n = 3) were photostimulated with 473 nm light (20 ms pulses) at three different frequencies (10,15, or 20 Hz) in three sweeps (5 s ON, 5 s OFF). The number of missed spikes were counted and the fraction of successful action potentials was plotted (A'). Efficient firing was observed in response to photostimulation at 10 and 15 Hz, but larger numbers of failures occurred at 20 Hz. This suggests 15 Hz as the maximal practical photostimulation rate for *Crfr2α*$^+$ChR2$^+$ cells, a frequency that also drove efficient picrotoxin (PTX)-sensitive postsynaptic inhibitory responses in downstream targets (B, B').

(C) Cell-attached recordings to test the ability of *Crfr2α*$^+$ChR2$^+$ neurons to be repetitively photostimulated. *top*, a single 2 ms flash of 473 nm light induced a rapid current response (latency < 1ms); (C') Photostimulation at 15Hz (2 ms pulse, 5 s ON) drove repetitive action currents (ACs) that were blocked by TTX. (C'') Extended photostimulation (15 Hz, 2 ms pulse, 5 s ON, 5 s OFF for 30 min) drove efficient firing with low failure rates throughout the recording in 5/6 neurons tested (C''').

(D) Stimulating *Crfr2α*$^+$ neurons during testing increases anxiety in the elevated plus maze. hrGFP(n = 14) versus ChR2(n = 16): entries in open arms (3.1 ± 0.6 versus 1.3 ± 0.4, $p < 0.05$), time in open arms (28.1 ± 6.0 versus 12.6 ± 3.7, $p < 0.05$).

(E) Stimulating *Crfr2α*$^+$ neurons during testing does not alter locomotor behavior. hrGFP(n = 39) versus ChR2(n = 38): Average velocity in the open field when animals were mobile (14.9 ± 1.3 versus 14.8 ± 0.8, $p > 0.9$).

(F) ChR2 expression in *Crfr2α*$^+$ neurons has no behavioral effects in the absence of 473 nm light. hrGFP (n = 12) versus ChR2(n = 12): LDB, entries in light side (9.0 ± 2.1 versus 9.3 ± 1.3, $p > 0.5$), time in light side (138.5 ± 42.7 versus 160.0 ± 31.2, $p > 0.5$); OF, entries in center (18.7 ± 2.4 versus 22.1 ± 3.7, $p > 0.4$), time in center (25.6 ± 4.7 versus 31.4 ± 4.4, $p > 0.3$); NO, entries in center (34.3 ± 3.9 versus 34.7 ± 2.8, $p > 0.9$), time in center (79.1 ± 13.3 versus 86.7 ± 12.0, $p > 0.6$).

(G) Stimulating *Crfr2α*$^+$ neurons does not alter locomotor behavior during subsequent testing. eYFP(n = 13) versus ChR2(n = 12): average velocity in the open field when animals were mobile (13.0 ± 0.3 versus 12.9 ± 0.4, $p > 0.8$).

(H) Retesting of mice 1 week after stimulation revealed no significant behavioral differences between groups. eYFP(n = 11) versus ChR2(n = 11): LDB, entries in light side (20.6 ± 2.7 versus 18.2 ± 1.5, $p > 0.4$), time in light side (220.7 ± 22.0 versus 257.8 ± 20.7, $p > 0.2$); OF(0–5′), entries in center (9.7 ± 1.0 versus 7.5 ± 1.5, $p > 0.2$), time in center (14.0 ± 2.3 versus 9.7 ± 1.9, $p > 0.15$); NO(0–5′), entries in center (12.0 ± 2.3 versus 9.0 ± 2.3, $p > 0.35$), time in center (22.3 ± 7.7 versus 18.5 ± 5.7, $p > 0.65$).

(I) Photostimulation of LS *Crfr2α*$^+$ neurons at 1 Hz is not sufficient to induce a persistent anxious state. eYFP(n = 13) versus ChR2(n = 14): LDB, entries in light side (7.2 ± 1.8 versus 4.5 ± 1.1, $p > 0.2$), time in light side (74.8 ± 23.6 versus 44.9 ± 13.6, $p > 0.25$); OF(0–5′), entries in center (7.2 ± 1.4 versus 4.5 ± 1.3, $p > 0.15$), time in center (7.2 ± 1.4 versus 5.5 ± 1.5, $p > 0.4$); NO(0–5′), entries in center (12.9 ± 3.4 versus 6.9 ± 2.5, $p > 0.15$), time in center (27.4 ± 7.6 versus 11.3 ± 6.3, $p > 0.10$). Values in (D)–(I) indicate mean ± SEM.

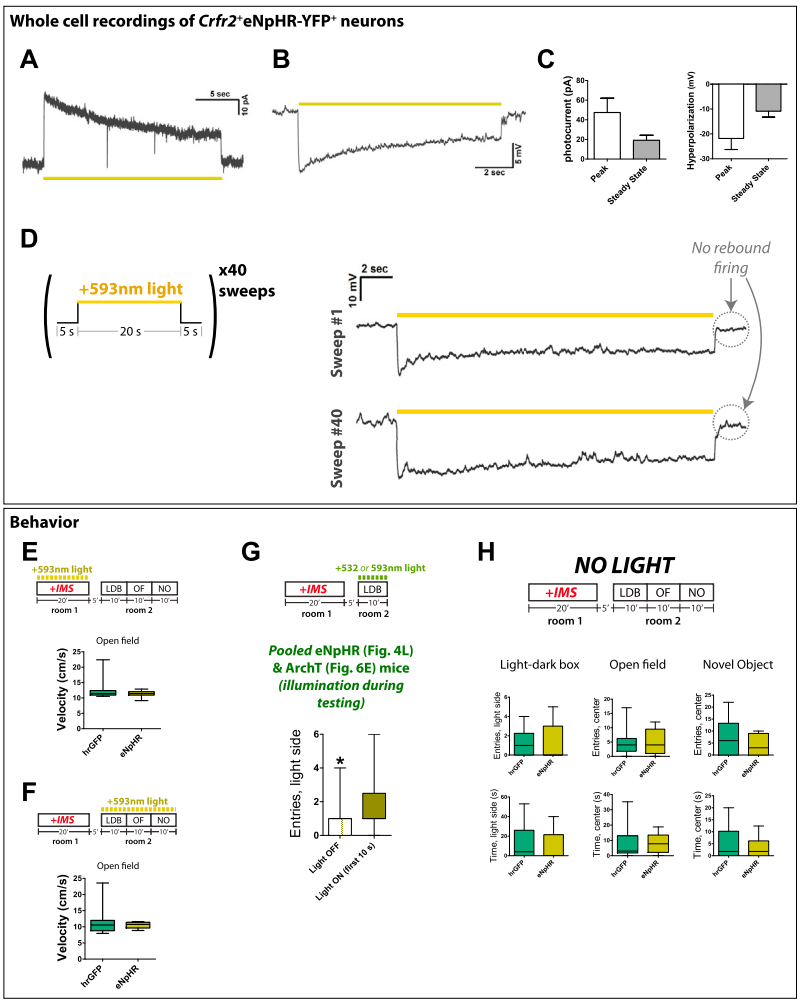

Figure S4. Photoinhibition of LS *Crfr2α*$^+$ Neurons and Controls for eNpHR2.0 Behavior Experiments, Related to Figure 4

(A–C) Whole cell voltage (A) or current (B) clamp recordings of eNpHR-YFP$^+$*Crfr2α*$^+$ neurons in response to 593 nm light (yellow lines) in LS slice preparations. (C) 59 nm light drove (*left*) outward currents (peak = 47.5 ± 14.6 pA; steady state = 19.2 ± 5.2 pA) and (*right*) hyperpolarization (peak = −21.8 ± 4.4 mV; steady state = −10.9 ± 2.4 mV) of moderate amplitudes. Values indicate mean ± SEM; n = 8 eNpHR-YFP$^+$ neurons recorded.

(D) To test whether repeated cycles of photoinhibition might lead to rebound firing (i.e., following hyperpolarization, membrane potential briefly rebounds to a more depolarized level than that prior to hyperpolarization, resulting in a transient increase in firing rate), *Crfr2α*$^+$eNpHR-YFP$^+$ neurons in whole-cell current clamp recording configuration were subjected to 40 sweeps of the following light protocol: 5 s light off, 20 s light ON, 5 s light OFF (*left*). In 3/3 cells, no significant rebound firing was observed, even after 20 min of repeated photoinhibition (*right*). Brief current injections performed at the completion of each sweep confirmed that the cells were healthy and capable of firing action potentials (data not shown).

(E) Inhibiting *Crfr2α*$^+$ neurons during IMS does not alter locomotor behavior during subsequent testing in the open field. hrGFP(n = 15) versus eNpHR (n = 17), data presented Mann-Whitney *U* value, *P* value: (*U* = 116.0, p > 0.65).

(F) Inhibiting *Crfr2α*$^+$ neurons during testing does not alter locomotor behavior in the open field. hrGFP(n = 11) versus eNpHR (n = 11), data presented Mann-Whitney *U* value, *P* value: (*U* = 46.5, p > 0.8).

(G) To test if low anxiety behavior might be more prevalent during light ON periods, we pooled together animals that received photoinhibition during testing which were injected with either eNpHR (cell body inhibition, Figure 4L) or ArchT (axon terminal inhibition, Figure 6E) and counted the number of entries made into the light side of the light-dark box during light OFF periods versus the first 10 s of light-ON periods. Due to small group sizes, eNpHR- or ArchT-injected mice alone yielded trends but not significant increases in low anxiety behavior during light ON periods (data not shown). In contrast, pooling both groups of mice together revealed a significant increase in entries made during light ON periods, indicating that the anxiolytic effects observed in response to optogenetic inhibition of *Crfr2α*$^+$ cell bodies or axons are not due to rebound effects during light OFF periods (n = 17), Wilcoxon matched-pairs signed rank test (p < 0.05). No significant difference in entries during light OFF versus ON periods was observed for control hrGFP expressing mice (n = 5), Wilcoxon matched-pairs signed rank test (p = 0.85) (data not shown).

(H) In the absence of 593 nm light, no differences between groups were observed hrGFP(n = 10) versus eNpHR (n = 9), data presented Mann-Whitney *U* value, *P* value: LDB, entries in light side (*U* = 41.5, p > 0.75), time in light side (*U* = 34.5, p > 0.6); OF, entries in center (*U* = 42.5, p > 0.85), time in center (*U* = 40.0, p > 0.7); NO, entries in center (*U* = 35.0, p > 0.4), time in center (*U* = 36.0, p > 0.7).

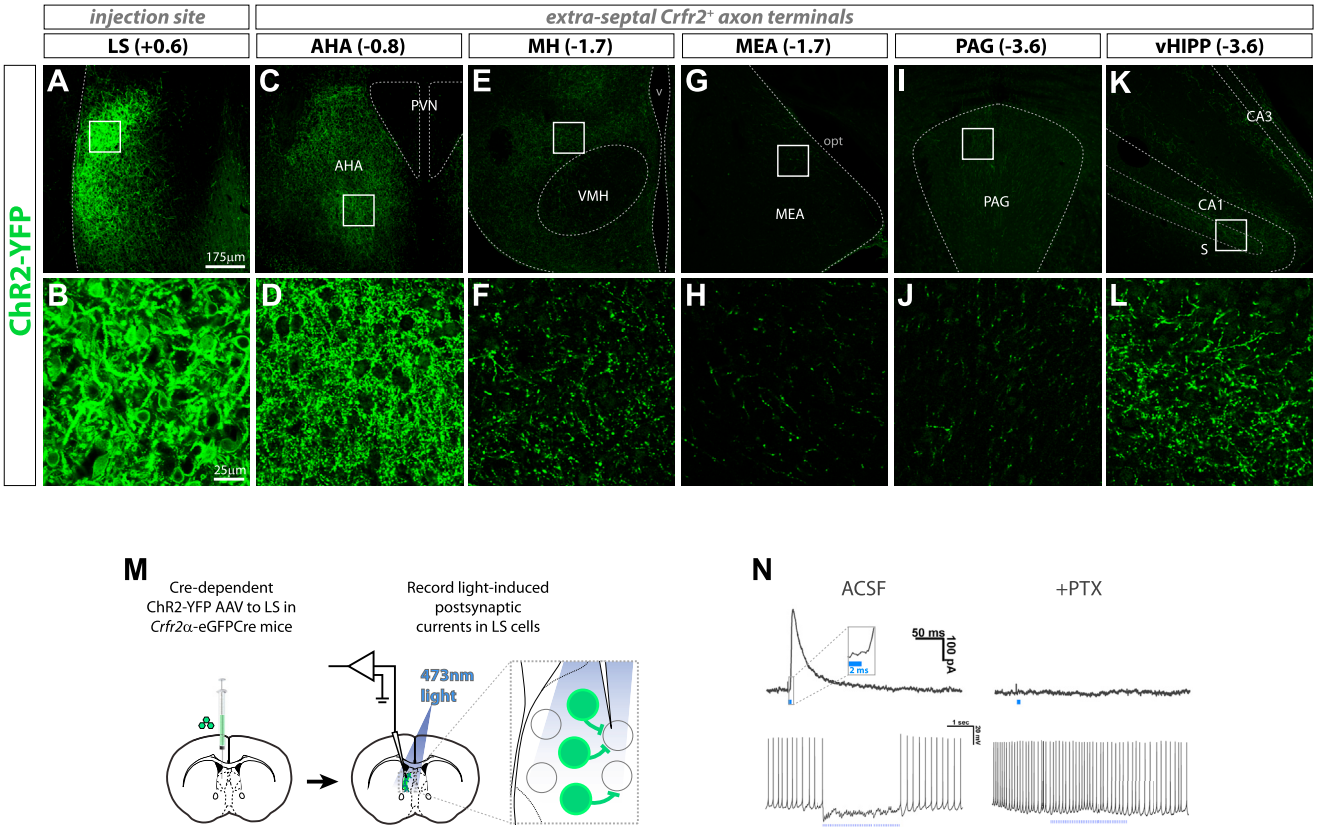

Figure S5. LS *Crfr2α*⁺ Neurons Send Projections to Multiple Extraseptal Targets and Make Local Inhibitory Synapses within the LS, Related to Figure 5

(A–L) Cre-dependent ChR2-YFP AAV was stereotaxically injected into the LS of *Crfr2α*-eGFPCre mice. After 4 weeks, analysis of YFP expression revealed robust fluorescence in the LS cell bodies and processes (A and B), as well as YFP⁺ axons in anterior hypothalamic area (AHA, C,D), more caudal regions of medial hypothalamus (MH, E and F), medial amygdala (MEA, G and H), periaqueductal gray (PAG, I and J), and ventral hippocampus (vHIPP, K,L). All extraseptal images were imaged on a confocal using the identical laser settings. Numbers in parentheses indicate bregma level; boxed regions in top panels are shown at higher magnification in bottom panels. PVN, paraventricular nucleus; VMH, ventromedial hypothalamic nucleus; opt, optic tract; CA1, CA3, fields CA1 or CA3 of hippocampus; S, subiculum. Locations of cell nuclei and layers were determined using DAPI counterstaining (data not shown).

(M) Schematic illustrating CRACM recordings, done by patching and recording photocurrents in ChR2-YFP-negative LS neurons that are near ChR2-YFP⁺ fibers.

(N) Single 2 ms pulses of 473 nm light evoked strong IPSCs in 9/9 cells (B, *top left*); average response amplitude = 241.1 ± 54.2pA; average responses latency = 4.7 ± 0.4 ms. *Bottom left*, 473 nm light delivered at 15 Hz (2 ms pulse width) was sufficient to inhibit induced firing of postsynaptic neurons. *Right*, both IPSCs (*top*) and IPSPs (*bottom*) were blocked by bath application of 100 μm picrotoxin.

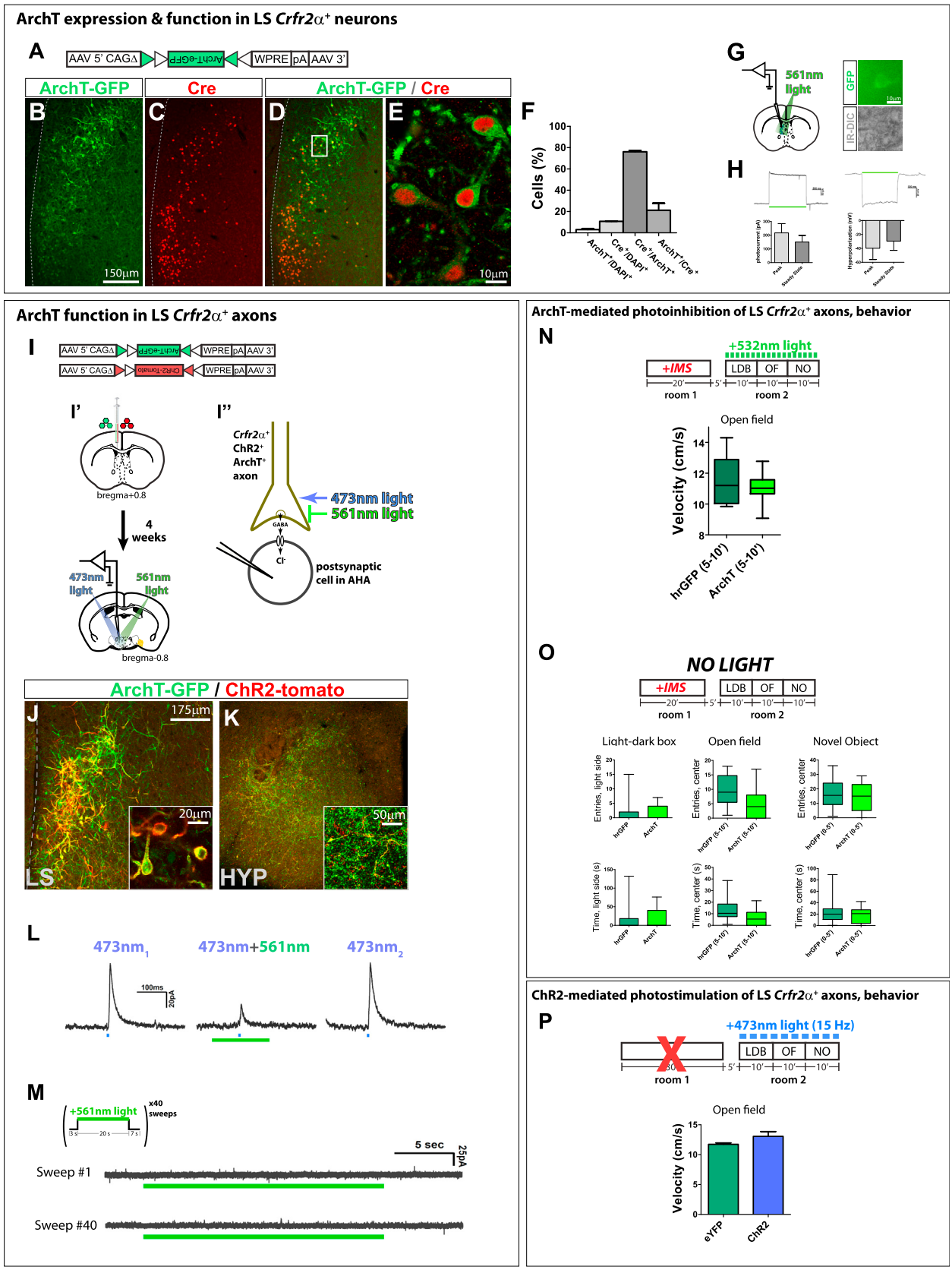

(legend on next page)

Figure S6. Photoinhibition and Photostimulation of LS *Crfr2α*$^+$ Axon Terminals in AHA, Related to Figure 6

(A) Cre-dependent ArchT-GFP AAV construct.

(B–E) Stereotaxic injection of (A) into the LS of *Crhr2α*-eGFPCre mice yielded ArchT-GFP (green) expression in *Crfr2α*$^+$ neurons (marked by Cre immunostaining, red). Boxed area in (D) shown at higher magnification in (E).

(F) Quantification of the specificity and sensitivity of recombination, counts were performed in regions containing ArchT-GFP$^+$ cells: ArchT$^+$/DAPI$^+$ = 3.0% ± 0.9%, Cre$^+$/DAPI$^+$ = 10.8% ± 0.2%, Cre$^+$/ArchT$^+$ = 76.1% ± 1.1%, ArchT$^+$/Cre$^+$ = 21.2% ± 6.6% (mean ± SEM). Total n = 7,253 DAPI$^+$ cells from 2 injected mice.

(G and H) Whole cell recordings of ArchT-GFP$^+$*Crfr2α*$^+$ neurons in LS slice preparations. (H) 532 nm light drove (*left*) outward currents (peak = 217. ± 67.5pA; steady state = 150.3 ± 48.7pA) and hyperpolarization (*right*) of large amplitude (peak = −39.9 ± 16.2 mV; steady state = −29.5 ± 13.3 mV). Values indicate mean ± SEM; n = 4 ArchT-GFP$^+$ neurons recorded.

(I) Diagram of experiment to test ArchT-GFP activity in axon terminals. Because no significant spontaneous activity of *Crfr2α*$^+$ neurons was detected in slice recordings (data not shown), we used an approach based on CRACM that enables optogenetic control over presynaptic release. (I') Two Cre-dependent constructs were coinjected into the LS of *Crfr2α*-eGFPCre mice to target expression of both ArchT-GFP and ChR2-tomato to *Crfr2α*$^+$ neurons. (I'') Postsynaptic neurons in the AHA were then patched and photostimulation of ChR2-tomato$^+$ArchT-GFP$^+$ axons with 473 nm light performed either in the absence or presence of 532 nm light. If ArchT-GFP is functional in axon terminals, the expectation is that it should be capable of suppressing ChR2-mediated IPSCs recorded from postsynaptic neurons.

(J and K) Coexpression of ArchT-GFP (green) and ChR2-Tomato (red) in LS (J) and hypothalamus (K) in a *Crfr2α*-eGFPCre mouse injected in LS with Cre-dependent AAVs encoding ArchT-GFP and ChR2-tomato.

(L) Voltage clamp recording of postsynaptic neuron in AHA from slice shown in (K). Photostimulation with a single 2 ms pulse of 473 nm light evoked IPSCs (left) that could be reversibly blocked by illumination with 532 nm light (middle, right). Traces shown are averaged responses of 5 trials.

(M) Repetitive photoinhibition of the cell shown in (L) over a 20 min period using the same 532 nm illumination protocol as that applied in vivo (20 s light ON, 10 s light OFF) did not produce detectable rebound activity in axon terminals following cessation of light.

(N) Inhibiting LS *Crfr2α*$^+$ axons in hypothalamus during testing does not alter locomotor behavior in the open field. hrGFP(n = 12) versus ArchT (n = 10), data presented Mann-Whitney *U* value, *P* value: (*U* = 42.0, p > 0.35).

(O) When light was not delivered through the guides, no significant differences in anxiety behavior were detected between groups. hrGFP(n = 12) versus ArchT (n = 11), data presented Mann-Whitney *U* value, *P* value: LDB, entries in light side (*U* = 60.0, p > 0.7), time in light side (*U* = 61.0, p > 0.7); OF, entries in center (5–10') (*U* = 35.0, p > 0.05), time in center (5–10') (*U* = 36.0, p > 0.05); NO, entries in center (0–5′) (*U* = 56.0, p > 0.5), time in center (0–5′) (*U* = 55.0, p > 0.5).

(P) Stimulating LS *Crfr2α*$^+$ axons in hypothalamus during testing does not alter locomotor behavior in the open field. eYFP(n = 17) versus ChR2 (n = 15), presented as mean ± S: average velocity in open field (11.73 ± 0.2 versus 13.1 ± 0.8, p > 0.1).

Note: In the NO assay, there was a trend toward increased anxiety (decreased number of entries on lighted side) that did not reach significance (Figure 6J). This may reflect a lower level of ChR2 present in nerve terminals (due to dilution during axonal transport). It is also possible that in the NO assay, a higher level of stimulation is required to overcome the appetitive influence exerted by the novel object, whereas no appetitive stimuli are present in the LDB and OF assays.

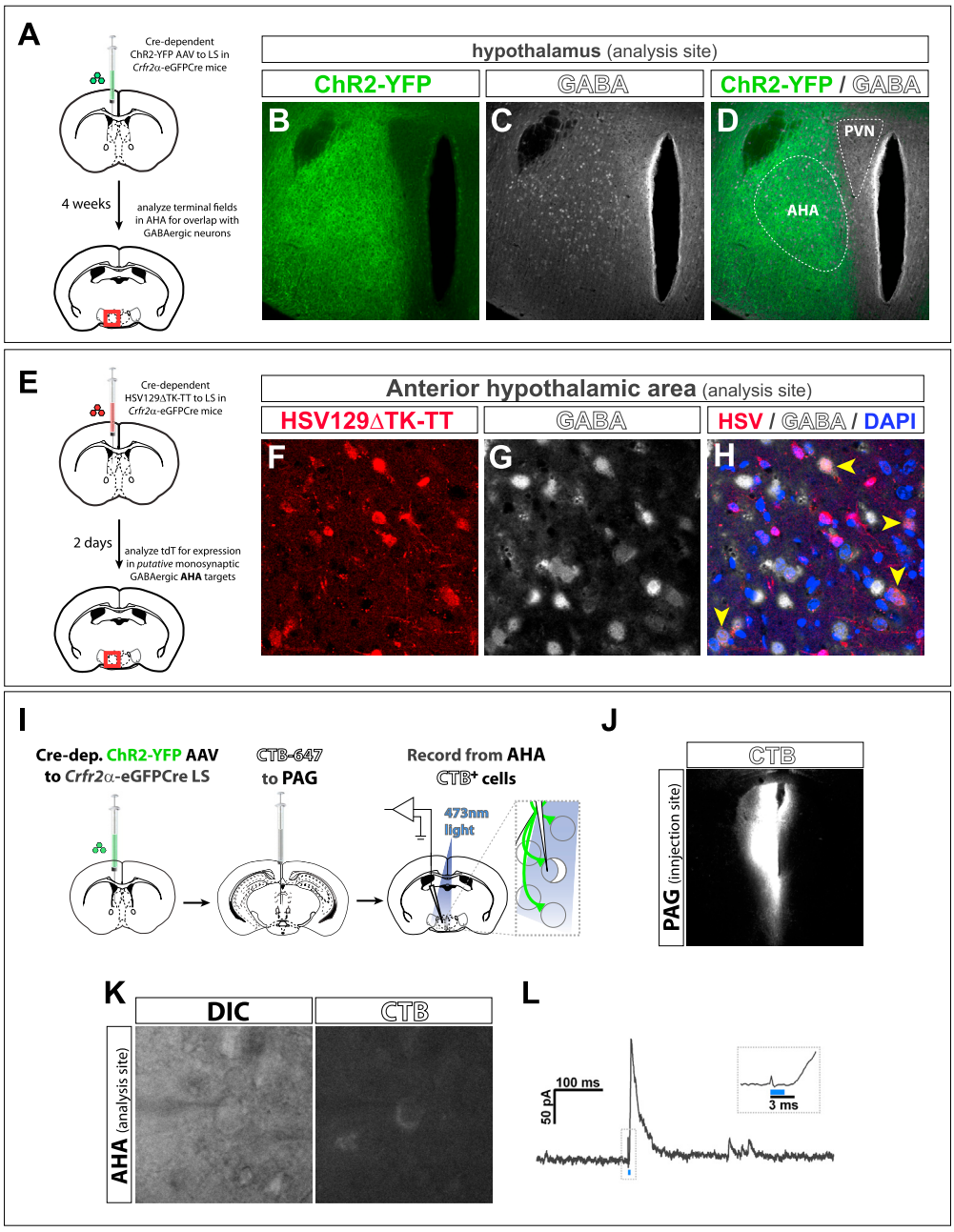

Figure S7. Evidence That LS *Crfr2α*$^+$ Neurons Monosynaptically Inhibit GABAergic Neurons in AHA and AHA Neurons that Innervate the PAG, Related to Figure 7

(A–D) LS *Crfr2α*$^+$ terminals overlap with GABAergic neurons in the AHA. Cre-dependent ChR2-YFP AAV was injected into the LS of *Crfr2α*-eGFPCre mice, yielding YFP labeling of axons (green, B,D) that are closely apposed to GABA$^+$ cells (white, C,D) in the AHA.

(E–H) The polysynaptic anterograde tracer HSV129ΔTK-TT was injected into the LS of *Crfr2α*-eGFPCre mice, and expression of tdTomato (red) and GABA (white) was analyzed 2 days later. This is a time point when transsynaptic transfer first becomes detectable in the hypothalamus and many labeled cells are thus likely to be monosynaptic targets (labeling in the PVN is not detected until 3 days postinjection). Consistent with the ChR2-YFP tracing, we observed tdT$^+$GABA$^+$ cells (F-H), suggesting that GABAergic neurons in the AHA are a target of LS *Crfr2α*$^+$ neurons.

(I–L) Combined CRACM and retrograde tracing demonstrate that LS *Crfr2α*$^+$ neurons monosynaptically inhibit AHA neurons that project to the PAG. (I) Schematic of experiment, in which Cre-dependent ChR2-YFP was injected into the LS of *Crfr2α*-eGFPCre mice and Alexa647-conjugated CTB was injected into the PAG. (J) This yielded strong CTB labeling at the site of injection (PAG) as well as in scattered backlabeled neurons throughout the AHA. (K,L) Single 2 ms pulses of 473 nm light evoked strong IPSCs in 4/5 CTB$^+$ cells in the AHA; average response amplitude = 74.7 ± 25.8pA; average responses latency = 4.1 ± 0.4 ms, consistent with monosynaptic connectivity.